

MODEL OF FRACTAL AGGREGATES INDUCED BY SHEAR

by

Zhanhong WAN^{a,b}, Jiawang CHEN^{a*}, Zhenjiang YOU^c, and Zhiyuan LI^a

^a Ocean College, Zhejiang University, Hangzhou, China

^b State Key Laboratory of Satellite Ocean Environment Dynamics, Hangzhou, China

^c ASP, University of Adelaide, Adelaide, SA, Australia

Original scientific paper
DOI: 10.2298/TSCI1305403W

It is an undoubted fact that particle aggregates from marine, aerosol, and engineering systems have fractal structures. In this study, fractal geometry is used to describe the morphology of irregular aggregates. The mean-field theory is employed to solve coagulation kinetic equation of aggregates. The Taylor-expansion method of moments in conjunction with the self-similar fractal characteristics is used to represent the particulate field. The effect of the target fractal dimensions on zeroth-order moment, second-order moment, and geometric standard deviation of the aggregates is explored. Results show that the developed moment method is an efficient and powerful approach to solving such evolution equations.

Key words: fractal dimension, aggregates, moment, coagulation

Introduction and kinetic aggregation physical models

The suspensions of fine solid particles or liquid droplets have been extensively observed both in nature and in industrial products, for example, air pollution such as smog and smoke, particle synthesis in flame reactor [1, 2], soot in flames, cement dust, etc. [3], and marine snow such as diatoms, fecal pellets, larvacean houses or miscellaneous materials [4]. The coagulation describing these types particulate aggregates is a fundamental process. Coagulation is the process that particles coalesce to form a bigger particle. Here coagulation may also refer to aggregation. The evolution of aggregates is sensitive to the history of particulates undergoing. The dynamic behavior of aggregates is described by a population balance equations (PBE). The coagulation dynamics is described by the well-known Smoluchowski's equation [5]:

$$\frac{\partial n}{\partial t} = \frac{1}{2} \int_0^{\infty} \beta(\tilde{v}, v - \tilde{v}) n(\tilde{v}, t) n(v - \tilde{v}, t) d\tilde{v} - \int_0^{\infty} \beta(\tilde{v}, v) n(\tilde{v}, t) n(v, t) d\tilde{v} \quad (1)$$

The first term of eq. (1) represents the formation of particle size v by collision of particles of size $v - \tilde{v}$ and \tilde{v} . The second term represents the loss of particle size v by collision with all other particles. The ratio of 1/2 in front of the first term is needed to avoid double counting. The collision kernel function $\beta(v, \tilde{v})$ describes the rate at which particles of size v coagulate with particles of size \tilde{v} . Coagulation bringing particles together are generally considered to be caused by three mechanisms: differential sedimentation, shear, and Brownian motion. Physical aggregation by the shear provides a fundamental mechanism, which presumably enhances open-ocean vertical fluxes of absorbed chemical species, fine lithogenic and biogenic material, and phytoplankton biomass following blooms in the marine environ-

* Corresponding author; e-mail: jiawang_chen@163.com

ments. Here the shear is simulated by the moments, but all other processes are also modeled by using this method of deterministic integration of their dynamic equations.

The rectilinear coagulation kernel β for shear is given by [6]. Numerical and physical experimentation has identified regimes of colloid aggregation that tends to produce porous aggregates of given fractal dimensions. In 3-D Euclidean space these aggregates are characterized by a fractal dimension, D_F :

$$\beta(v, \tilde{v}) = k_s \frac{G}{\pi} v_0^{1-\frac{3}{D_F}} \left(\frac{1}{v^{D_F}} + \frac{1}{\tilde{v}^{D_F}} \right)^3 \quad (2)$$

k_s is equal to 1.0 and 0.975 for laminar and turbulent shear, respectively. The mean shear rate G is given by velocity gradient for laminar shear and is given in terms of the dissipation rate ε and kinematic viscosity ν in the turbulent flow.

The most employed general method and its variants for solving the PBE (1, 2) is based on dividing the particle size domain into sections as developed by Gelbard *et al.* [7]. However, these direct discretization methods encounter various problems for either coagulation or other dominated dynamic processes, for example, numerical error in specifying a given distribution in a section, non-positiveness and non-conservation of mass and number concentration due to numerical diffusion. The widely used alternative approach is the method of moments [8, 9], which solves a group of moments equations derived from the PBE. The Taylor-expansion moment method [10-13] has been applied to solve fractal aggregation of the Brownian motion. Here we extended to close the PGDE equation by invoking fractal theory and apply it to shear process. The k^{th} ($k = 0, 1, 2, \dots$) order moment is defined as:

$$M_k = \int_0^\infty v^k n(v, t) dv \quad (3)$$

Therefore, M_0 indicates the particle number density, M_1 the diameter density, and M_2 the surface area density, *etc.* The dynamic equations for the moment set are obtained by applying the moment transformation to the GDE, *i. e.*, multiplying by v_k and integrating over the entire particle size distribution space, and finally the transformed moment equation is rendered:

$$\begin{aligned} \frac{dM_0}{dt} = & -k_s \frac{G}{2\pi} v_0^{1-\frac{3}{D_F}} \frac{1}{D_F^4 M_1^2} \left(\frac{M_1}{M_0} \right)^{\frac{3}{D_F}-2} \left[6(-2 + 3D_F + 3D_F^2 - 2D_F^3) M_0 M_1^2 M_2 + \right. \\ & \left. + (6 - 9D_F - 21D_F^2 + 12D_F^3 + 8D_F^4) M_1^4 + 3(2 - 3D_F + D_F^2) M_0^2 M_2^2 \right] \end{aligned} \quad (4)$$

$$\begin{aligned} \frac{dM_2}{dt} = & k_s \frac{G}{2\pi} v_0^{1-\frac{3}{D_F}} \frac{2}{D_F^4 M_1^2} \left(\frac{M_1}{M_0} \right)^{\frac{3}{D_F}} \left[6(-2 - 3D_F + 3D_F^2 + 2D_F^3) M_0 M_1^2 M_2 + \right. \\ & \left. + (6 + 9D_F - 21D_F^2 - 12D_F^3 + 8D_F^4) M_1^4 + 3(2 + 3D_F + D_F^2) M_0^2 M_2^2 \right] \end{aligned} \quad (5)$$

It should be pointed out that this approach has no prior requirement for particle size spectrum, and the limitation existing in the log-normal distribution theory automatically disappears as other moment methods. The whole derivation of the equations does not involve any assumptions for particle size spectrum, while the final form of equation system is much simpler than, for example, that from the PMM model [14].

Results and discussion

The numerical computations are all performed on an Intel (R) 4 cores CPU computer with memory 4 GB. The fourth-order Runge-Kutta method with fixed time step is used to solve the system of differential equations. In the computations, all the numerical simulations are based on the dimensionless time, and the time step is supposed to be small enough, 0.001, in order to achieve an accurate result.

Theoretically, the aggregates fractal dimension can vary from the 1-D of initial line array of particles to 3-D of particles forming sphere. Clark and Flora [15] summarized the results of aggregates structure fractal dimension and found that the fractal dimension varied approximately from 1.6 to 2.8 is universal (with values between 1.9 and 2.3 reported in the literature and references within). Therefore, in the present work, the values of fractal dimension changes in this regime. In order to make comparison, the first calculation is performed using the same data as of Spicer and Peatsinis [16] *i. e.*, the initial particle diameter $d_0 = 2.17 \mu\text{m}$, the initial particle number concentration $N_0 = 9.3 \cdot 10^6 \text{ cm}^{-3}$, and the shear rate $G = 50 \text{ s}^{-1}$. It can be seen from fig. 1(a), with the increase of dimensionless time, $\tau = G\phi_0 t$, due to the particle aggregate, particle number concentration decreases gradually, so the zeroth-order moment decreases. For a given fractal dimension, there is an obvious inflection point in the zeroth-order moment curve. Meanwhile, the greater the fractal dimension is, namely the denser the aggregates body is, the longer the aggregation time become. From the point of view of the physical mechanism, the smaller the fractal dimension, the looser the aggregates assembled by small particles, the bigger the accessible surface area, the larger the chance for other particles to contact with it, so the faster the aggregates formation, the shorter the aggregation time. The inflection on the curve corresponds to the critical situation of aggregates.

The second-order moment as a function of time under the condition of different fractal dimension is shown in fig. 1(b). For a given fractal dimension, as the time develops, the second-order moment will also increase with aggregation time. Meanwhile, the increase of fractal dimension can reduce the second-order moments. Physically, the second-order moment is proportional to composition systems of particle surface. So, the change of second-order moment is the same as the change of particle total surface per unit volume of fluid. Therefore, the total surface of particles decreases with the increase of fractal dimension.

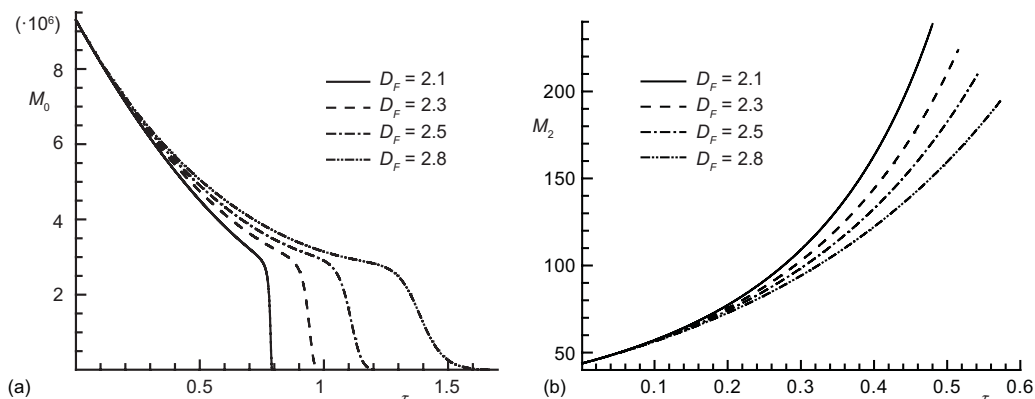


Figure 1. The k^{th} moments along time; (a) M_1 , (b) M_2

The geometric standard deviation of aggregates size distribution can quantitatively describe the distribution width.

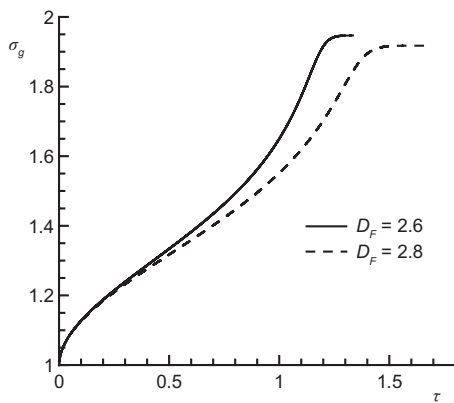


Figure 2. The curve of σ_g changes with D_F

It can be seen that for different initial particle concentrations, the relations between the second-order moment and the time are identical, while the changes of zeroth-order moment are different. When the initial particle concentration is large, the probability of particle collision increases, and the aggregate rate rises. Therefore, the particle concentration decreases faster at the beginning. However, the geometric standard deviation is not affected by the initial particle concentration (fig. 5).

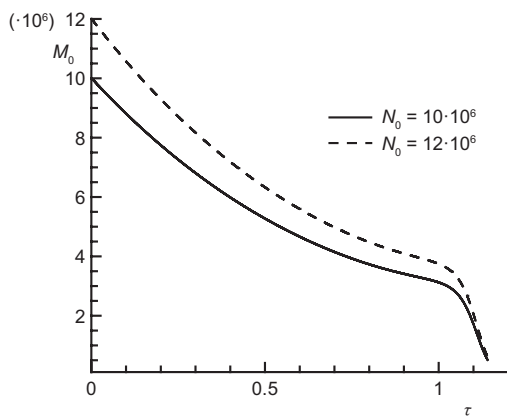


Figure 3. The curve of M_0 changes with time τ

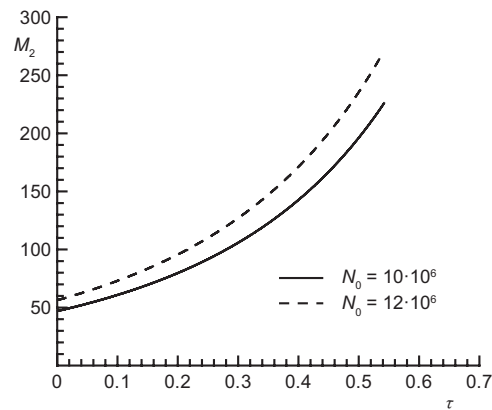


Figure 4. The curve of M_2 changes with time τ

Given the initial particle concentration $N_0 = 9.3 \cdot 10^6 \text{ cm}^{-3}$, the curves of zeroth-order moment, second-order moment and geometric standard deviation changing with time under the condition of different initial particle diameters are shown in figs. 6-8. Different from varying the initial particle concentration, changing initial particle diameter has no apparent effects on the zeroth-order moment and geometric standard deviation. While the second-order moment changes significantly, due to the increase of initial particle diameter.

Conclusions

We used the Taylor-series expansion technique to dispose the collision terms for shear motion and the fractional moments. Other than solving the discretized PBE, the present used alternative approach solves a group of moments equations derived from the PBE. These

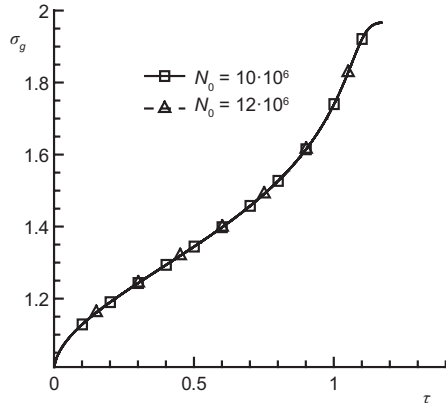


Figure 5. The curve of σ_g changes with time τ

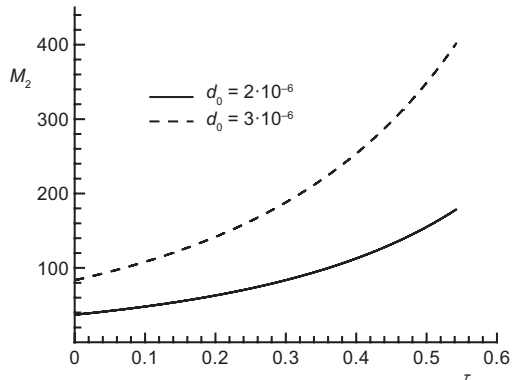


Figure 6. The curve of M_2 changes with time τ

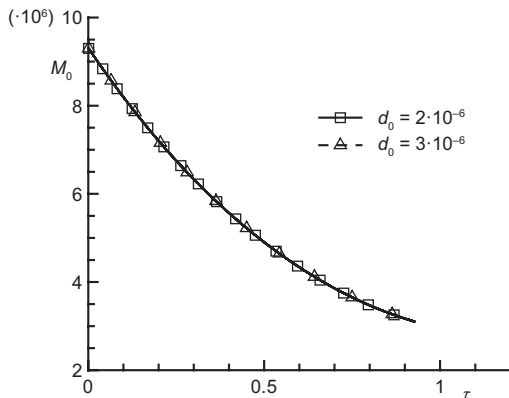


Figure 7. The curve of M_0 changes with time τ

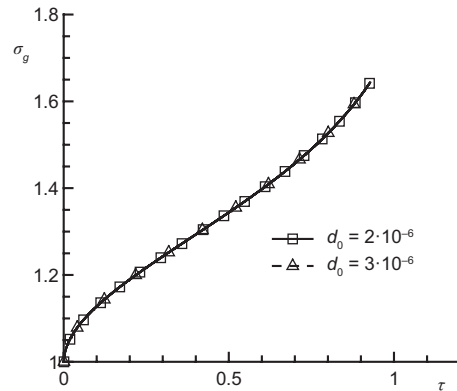


Figure 8. The curve of σ_g changes with time τ

moments (several low order moments) provide important information on the PSD function, *i. e.*, number density, volume fraction, polydispersity, *etc.* However, owing to the non-linearity of the PBE, the governing equations for lower order moments contain higher order moments, which are not closed after cutting off. We have developed our previous study [17] and obtained a new closure form for the moment equations incorporating fractal theories.

The results show that the effects of fractal dimension on the zeroth-order moment, second-order moment and geometric standard deviation are examined, the mechanisms of fractal dimension are analyzed, and the relations between aggregate structure parameters and fractal dimension are obtained. Similar to the Brownian aggregation [17], in flow shear aggregation, the particle size still has the self-holding characteristic. The initial particle size and initial concentration have no effects on the final size distribution. With the increase of fractal dimension, the geometric standard deviation which reflects the self-holding reduces gradually. At the same, the simplicity and high accuracy of this closure makes it available to accommodate other complex physical collision kernel models for coagulation dynamics with high flexibility.

Acknowledgments

The Support by the Public Science and Technology Research Funds Projects of Ocean (NO. 201205015), the National Natural Science Foundation of China (NO.10902097) and the Natural Science Fund of Zhejiang Province (NO. Y6090257) is gratefully acknowledged.

Nomenclature

n – particle size distribution density function, [$\text{cm}^3\text{cm}^{-3}$]
 t – time, [s]
 M_k – k^{th} moment of size distribution
 D_F – fractal dimension
 G – shear rate, [s^{-1}]
 v_0 – volume of primary particle, [cm^3]
 v, \square – particle volume, [cm^3]

Greek symbols

ϕ – volume fraction of aggregates
 σ_g – geometric standard deviation

Subscripts

0 – referred to initial condition
 a – aggregate

References

- [1] Yu, M. Z., *et al.*, Numerical Simulation of Nanoparticle Synthesis in Diffusion Flame Reactor, *Powder Technol.*, 181 (2008), 1, pp. 9-20
- [2] Yu, M. Z., *et al.*, Effect of Precursor Loading on Non-Spherical TiO_2 Nanoparticle Synthesis in a Diffusion Flame Reactor, *Chem. Eng. Sci.*, 63 (2008), 9, pp. 2317-2329
- [3] Friedlander, S. K., *Smoke, Dust and Haze: Fundamentals of Aerosol Behavior*, John Wiley and Sons, New York, USA, 2000
- [4] Logan, B. E., Wilkinson, D. B., Fractal Dimensions and Porosities of Zoogloeamyces and Saccharomyces Cerevisiae Aggregates, *Biotechnol. Bioeng.*, 38 (1991), 8, pp. 389-396
- [5] Kostoglou, M., *et al.*, Bivariate Population Dynamics Simulation of Fractal Aerosol Aggregate Coagulation and Restructuring, *J. Aerosol Sci.*, 37 (2006), 9, pp. 1102-1115
- [6] Jiang, Q., Logan, B. E., Fractal Dimensions of Aggregates from Shear Devices, *J. Am. Water Works Assoc.*, 88 (1996), 2, pp. 100-113
- [7] Gelbard, F., *et al.*, Sectional Representations for Simulating Aerosol Dynamics, *J. Colloid Interf. Sci.*, 76 (1980), 2, pp. 541-556
- [8] McGraw, R., Description of Aerosol Dynamics by the Quadrature Method of Moments, *Aerosol Sci. Technol.*, 27 (1997), 2, pp. 255-265
- [9] Marchisio, D. L., Fox, R. O., Solution of Population Balance Equations Using the Direct Quadrature Method of Moments, *J. Aerosol Sci.*, 36 (2005), 1, pp. 43-73
- [10] Yu, M. Z., *et al.*, A New Moment Method for Solving the Coagulation Equation for Particles in Brownian Motion, *Aerosol Sci. Technol.*, 42 (2008), 9, pp. 705-713
- [11] Zhou, K., Monte Carlo Simulation for Soot Dynamics, *Thermal Science*, 16 (2012), 5, pp. 1391-1394
- [12] Lin, J. Z., *et al.*, Research On The Transport and Deposition of Nanoparticles in a Rotating Curved Pipe, *Phys. Fluids*, 21 (2009), 12, pp. 11
- [13] Yu, M., *et al.*, The Verification of the Taylor-Expansion Moment Method for the Nanoparticle Coagulation in the Entire Size Regime due to Brownian Motion, *J. Nanopart. Res.*, 13 (2011), 5, pp. 2007-2020
- [14] Park, S. H., Lee, K. W., Change in Particle Size Distribution of Fractal Agglomerates during Brownian Coagulation in the Free-Molecule Regime, *J. Colloid Interf. Sci.*, 246 (2002), 1, pp. 85-91
- [15] Clark, M. M., Flora, J. R. V., Floc Restructuring in Varied Turbulent Mixing, *J. Colloid Interf. Sci.*, 147 (1991), 2, pp. 407-421
- [16] Spicer, P. T., Pratsinis, S. E., The Evolution of Floc Structure and Size Distribution during Shear-Induced Flocculation, *Water Res.*, 30 (1996), 5, pp. 1046-1056
- [17] Wan, Z. H., *et al.*, Method of Taylor Expansion Moment Incorporating Fractal Theories for Brownian Coagulation of Fine Particles, *Int. J. Nonlinear Sci. Numer. Simul.*, 13 (2012), 7-8, pp. 459-567

Paper submitted: January 18, 2013

Paper revised: April 26, 2013

Paper accepted: May 1, 2013